BER the international journal of bridge engineering management and research

Load Testing and Rating of Simple-Span Prestressed Concrete Bridges with no Record Plans

Osman Hag-Elsafi[1*]; Jonathan Kunin[2] and Sreenivas Alampalli[3]

Submitted: 14 April 2026 **Accepted:** 24 June 2026 **Publication date:** 10 July 2026

DOI: 10.70465/ber.v3i3.91

Abstract: This paper introduces a pioneering approach for load testing and rating of simple-span prestressed concrete bridges when design information about the structure is not available. The paper uses the testing of a bridge in New York for illustration of the proposed approach. The bridge was built in 1961 and consisted of five simply supported 70-ft-long post-tensioned bulb-T beams. No documents or plans for the structure were available at the time of the testing. In 1970, the structure was posted for 12 tons. The absence of the bridge plans, coupled with the public's demand to accommodate school bus traffic on the bridge, prompted the load testing and rating. A plan based on an assumed design basis and investigation of bridge behavior under controlled truck loading was proposed to determine unknown design parameters and enable load rating of the structure. The bridge was then instrumented and load tested using trucks of known weights and configurations, positioned at specified locations on the deck to gradually increase their safe load effects on the structure. The results of the testing provided the required information about the bridge and allowed for load rating of the structure.

Author keywords: Prestressed concrete bridges; post-tensioned bridges; load testing; load distribution; bridge evaluation; load rating

Introduction

Bridge rating is routinely conducted by load rating engineers to evaluate and update the load carrying capacities of bridges. The rating process combines the knowledge gained during inspection cycles, which accounts for in-service condition, with appropriate analysis to determine load rating, namely, Inventory and Operating.[1] Load ratings based on the inventory level allow comparisons with the capacity for new structures and, therefore, result in a live load, which can safely utilize an existing structure for an indefinite period of time.[1] Load ratings based on the operating rating level generally describe the maximum permissible live load to which the structure may be subjected. Allowing unlimited numbers of vehicles to use the bridge at the operating level may shorten the life of the bridge.[1] Using these ratings, transportation agencies often apply their own policies to determine a structure's safe load-carrying capacity, which may result in allowing legal traffic on the bridge, posting a load limit on the structure, or restricting the bridge to certain types of permit loads. Most of the time there is a high degree of confidence in the parameters that influence the load-carrying capacity evaluation (such as the section properties of structural members, material strengths, and physical characteristics) to conduct an analytical rating. However, occasionally, these parameters cannot be adequately estimated/accounted for, and a test-based rating is warranted for a more realistic appraisal of the structure's load-carrying capacity. This is the typical situation for the application of testing for bridge load rating.[2–7] A more challenging situation arises when the bridge targeted for the load rating is a prestressed structure with no plans on record. An approach for load testing and rating of such structures is presented in this paper, using an actual load test performed on a bridge in New York State (NYS). Prestressed concrete bridges of unknown design records are not unique to any specific state and do exist in the inventory of many bridge owners all around the globe. This fact gives credence to the pioneering approach presented in this paper as a viable tool for all prestressed concrete bridge owners. This is especially true given that very few studies of this nature were conducted in the United States.[8–10] All these studies included approaches that combined a semi-theoretical basis for design with diagnostic or proof load testing. Texas Department of Transportation assigns HS-15 and HS-20 Inventory and Operating Ratings, respectively, for reinforced concrete bridges with no record plans that show no signs of structural stress. For bridges

*Corresponding Author: Osman Hag-Elsafi.
Email: Osman.Hag-Elsafi@dot.ny.gov
[1]Structure Management Bureau, Office of Structures, New York State Department of Transportation, 50 Wolf Road, Albany, NY 12232
[2]Technical Services Division, New York State Department of Transportation, 50 Wolf Road, Albany, NY 12232
[3]CEO, Alampalli Engineering, PLLC, 9 Stedman Way, Albany, NY 12211

Discussion period open till six months from the publication date. Please submit separate discussion for each individual paper. This paper is a part of the Vol. 3 of the International Journal of Bridge Engineering, Management and Research (© BER), ISSN 3065-0569.

older than 4 years that meet additional NBI ratings criteria, the structure may be load-posted at the Inventory level.[11] Oregon Department of Transportation assigns a rating factor of 1.0 for bridges in fair or better National Bridge Inventory (NBI) condition when long-term performance demonstrates their ability to carry legal loads. Inventory and Operating Ratings are estimated by considering the specific NBI condition ratings.[12]

The paper introduces a pioneering approach for the load rating of simple-span prestressed concrete bridges when there are no record plans. It discusses how load testing could be performed for load rating of simple-span prestressed concrete structures when there are no plans on record, using an actual bridge structure for illustration. It starts with background information on the structure, followed by a description of the preliminary analysis required for determining safe loads that could be applied during the testing, plans for instrumentation, load testing and results, load rating analysis, and conclusions.

Test Structure

The structure (Fig. 1) carried Dean's Mill Road over Hannacrois Creek near the Town of New Baltimore in Greene County, New York. The bridge was built in 1961 and made of 5 post-tensioned concrete bulb-T beams with 8-in. wide closure pours between the beams and an asphalt overlay riding surface.

In 1970, a load posting of 12 tons was placed on the bridge. No bridge plans or documentation of the load posting were available. Hence, preliminary analysis to estimate the capacity of the prestressed beams was performed using the 1961 edition of the AASHTO Standard Specifications for Highway Bridges.[7] Among the important revisions in this edition were the sections on Prestressed Concrete, which were based largely on the report of the Joint ASCE-ACI Committee on Prestressed Concrete of 1958 and used as Tentative Specifications for 2 years.

Instrumentation and load test plans were first developed, and the bridge was instrumented with strain gages in preparation for the load testing.

Preliminary Analysis

Analysis of the bridge structure conducted prior to the load testing targeted:

1. Identification of the beams' design parameters.
2. Estimation of ultimate and cracking moment capacities.
3. Determination of the maximum load that can be safely applied during the testing.
4. Estimation of expected strains under the maximum load determined above.

Identification of the design parameters was important to determine the tolerable stresses that will be used in the load rating equations. Ultimate and cracking moments are needed to determine the safe load to be applied during the testing, and the strain induced by this load is an important trigger to watch for during the testing. In the absence of the bridge plans, field measurements of the structure's critical dimensions could be made to determine section properties and estimate dead loads. The contribution of parapets, sidewalks, and other attachments to the stiffness of the structure could be ignored.

Beam Analysis

A typical beam was analyzed using Mathcad programming (Beam section in Fig. 1b). The analysis was performed assuming the beam was designed to satisfy the 1961 AASHTO requirements on initial and final stresses.[7] Section

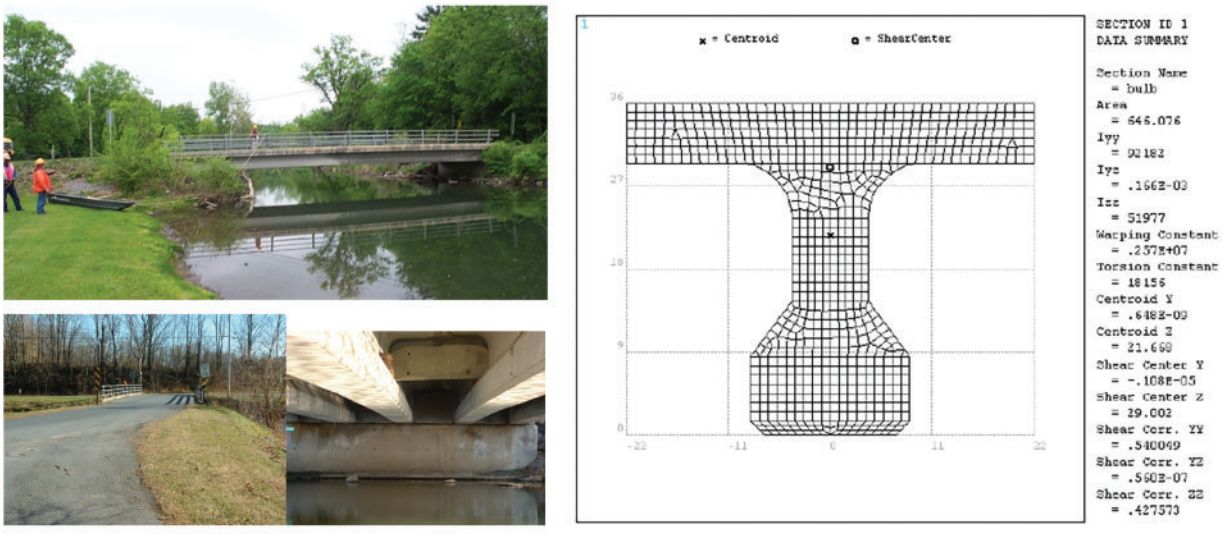

Figure 1. (a) Bridge views. (b) Typical beam section and properties

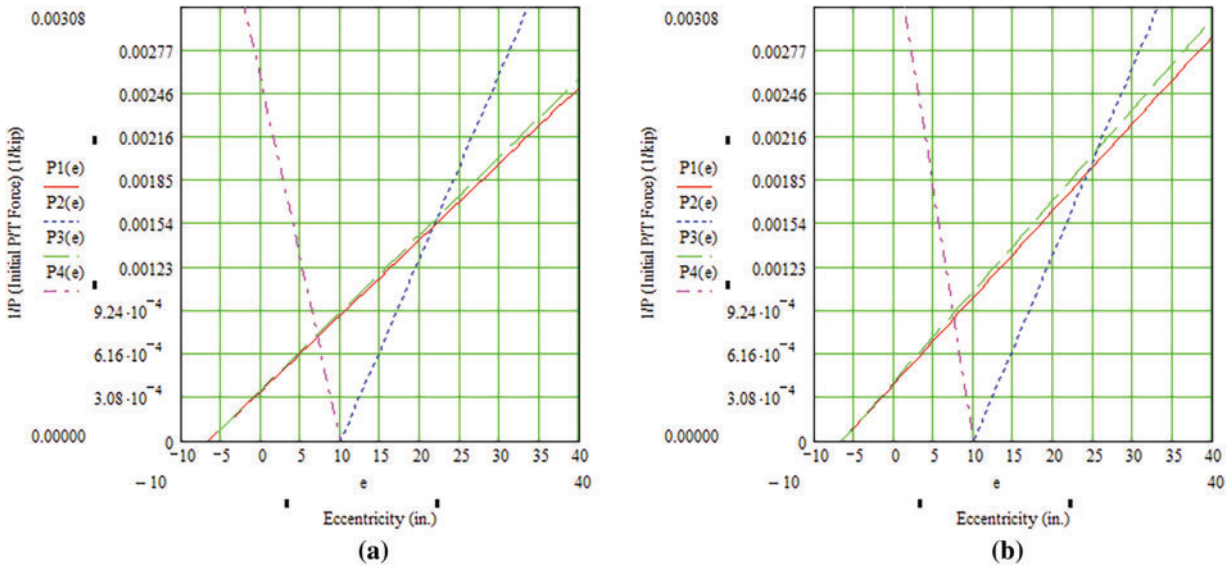

Figure 2. Feasible solution for AASHTO H-20 and HS-20 loading

properties were calculated based on measured beam dimensions. Dead load moment was calculated using the weight of the beam, closure pours, guide rails, and asphalt overlay (Total dead load moment $M_{DL} = 522$ kip-ft). Live load moment was calculated assuming the bridge was designed for an AASHTO HS-20 or H-20 loading, using a distribution factor of S/5, where S is the beam spacing (4 ft 4 in.), and an impact factor of 1.26 (respective design moments, $M_{HS\text{-}20} = 535.9$ or $M_{H\text{-}20} = 384.9$ kip-ft).[1,7,8]

Assumptions

The structure is assumed to meet the following minimum code requirements:

1. Compressive strength of concrete at 28 days $f_c' = 5000$ psi.
2. Compressive strength of concrete at time of initial prestress $f_{ci}' = 4000$ psi.
3. Modulus of elasticity of concrete $E_c = 57000\sqrt{f_c'}$.
4. Ultimate strength of post-tensioning steel $f_s' = 240$ ksi.
5. Nominal yield point stress of prestressing steel at 1% extension $f_{sy} = 192$ ksi.
6. Modulus of elasticity of steel $E_s = 29000$ ksi.

Allowable Stresses

The following allowable stresses were used in the program:

1. Temporary stresses in the steel before losses due to creep and shrinkage $= 0.7\ f_s'$.
2. Steel stress at design load (after losses) = the smaller of $0.6\ f_s'$ or $0.8\ f_{sy}$.
3. Temporary compressive stresses in concrete before losses due to creep and shrinkage $= 0.55\ f_{ci}'$.
4. Temporary tensile stresses in concrete before losses due to creep and shrinkage $= 3\sqrt{f_{ci}'}$
5. Concrete compressive stress after losses have occurred $= 0.4\ f_c'$.
6. Concrete tensile stress after losses have occurred = 0.
7. Concrete cracking stress $f_{Cracking} = 7.5\sqrt{f_{ci}'}$.

Prestress Losses

Prestress losses were calculated based on:

1. Post-tensioning steel stress losses due to all causes except friction = 25 ksi.
2. Post-tensioning steel stress losses due to friction $= 0.15 \times 0.7\ f_s'$.

Ultimate Moment Capacity

The ultimate moment capacity of the beam was calculated by first confirming that the neutral axis was located inside the top flange. This is usually the case when the flange thickness calculated using $t_{flange} = 1.4\dfrac{d\rho f_{su}}{f_c'}$ is greater than the actual flange thickness t (t = 6.5 in.). The following equations:

$$M_u = A_{sr} f_{su} d\left(1 - 0.6\frac{A_{sr} f_{su}}{b'\ \mathrm{d}\ f_c'}\right) + 0.85 f_c'\left(b - b'\right) t\,(d - 0.5t) \quad (1)$$

where

$$A_{sr} = A_s - A_{sf} \quad (2)$$

is the steel area required to develop the ultimate compressive strength of the web.

$$A_f = 0.85 f_c'\left(b - b'\right) t / f_c' \quad (3)$$

Table 1. Beam analysis for selected P_i and e combinations

Parameter	HS-20		H-20	
	High P/T	Low P/T	High P/T	Low P/T
$1/P_i \times 10^{-4}$ (1/kip)	7.38	13.96	9.00	16.28
P_i (kip)	1355.00	716.50	1111.00	614.40
e (in.)	7.10	18.7	7.75	18.68
P_e (kip)	949.86	502.27	778.81	430.69
A_s (in.^{2})	8.07	4.27	6.61	3.67
$M_u \times 10^4$ (kip-in.)	2.65	3.14	2.27	2.62
$M_{Fact.} \times 10^4$ (kip-in.)	2.55	2.55	2.09	2.09
$M_{cr} \times 10^4$ (kip-in.)	1.55	1.52	1.34	1.31
$M_{Test} \times 10^3$ (kip-in.)	9.21	8.90	7.16	6.88
f_{Test} (ksi)	2.17	2.09	1.68	1.62
Δ (in.)	1.33	1.285	1.132	1.09

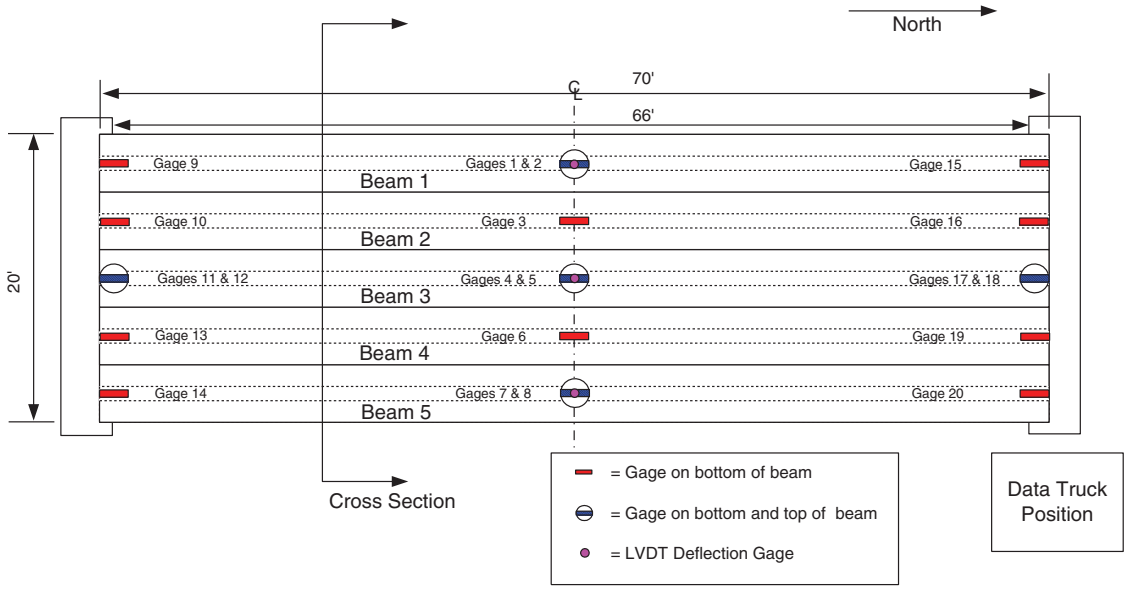

Figure 3. Instrumentation plan

is the steel area required to develop the ultimate capacity of the overhanging portion of the flange. The steel stress f_{su} is estimated using the following equation:

$$f_{su} = f_s' \left(1 - 0.5\frac{\rho f_s'}{f_c'}\right) \tag{4}$$

which is also subject to the condition that the effective prestress after losses is not less than 0.5 f_s'.

Cracking Moment

Cracking moment was calculated using

$$M_{Cracking} = S_b \left[P_e \left(\frac{1}{A} + \frac{e}{S_b}\right) + f_{Cracking}\right] \tag{5}$$

where S_b is the section modulus for the beam bottom, P_e is the effective prestress force, A is the beam cross-sectional area, e is the post-tensioning steel eccentricity, and $f_{Cracking}$ is previously defined.

Maximum and Minimum Steel Percentages

The maximum percentage of steel used in the analysis was 0.3 percent and the minimum percentage was calculated using

$$\rho_{\min} = A_{sr}\frac{f_{su}}{b' \, \mathrm{d} \, f_c'} \tag{6}$$

Feasible Solutions for Initial Prestress Force and Eccentricity

The analysis consisted of determining feasible solutions for the reciprocal of the initial prestressing force and eccentricity

using a linear programming approach. In this approach, the four inequalities relating the reciprocal of the initial post-tensioning force and eccentricity were first formulated, based on satisfying the code requirements for midspan top and bottom stresses under initial and service load conditions, and then plotted to determine the region of feasible solutions. The four inequalities were formulated as follows:

$$
\begin{aligned}
P1(e) &\geq \frac{1}{A \cdot \left(f_{bi} + \frac{M_{DL}}{S_b}\right)} + \frac{e}{S_b \cdot \left(f_{bi} + \frac{M_{DL}}{S_b}\right)} \\
P2(e) &\leq \frac{-1}{A \cdot \left(f_{ti} + \frac{M_{DL}}{S_t}\right)} + \frac{e}{S_t \cdot \left(f_{ti} + \frac{M_{DL}}{S_t}\right)} \\
P3(e) &\leq \kappa \left[\frac{1}{A \cdot \left(-f_{bf} + \frac{M_{Tot}}{S_b}\right)} + \frac{e}{S_b \cdot \left(-f_{bf} + \frac{M_{Tot}}{S_b}\right)} \right] \\
P4(e) &\geq \kappa \left[\frac{-1}{A \cdot \left(-f_{tf} + \frac{M_{Tot}}{S_t}\right)} + \frac{e}{S_t \cdot \left(-f_{tf} + \frac{M_{Tot}}{S_t}\right)} \right]
\end{aligned}
\tag{7}
$$

where P1(e) and P2(e), respectively, were based on satisfaction of midspan bottom and top stresses under initial prestressing force and before prestressing losses take place. P3(e) and P4(e), respectively, were based on satisfaction of midspan bottom and top stresses under final prestressing force and after prestressing losses take place. e is the prestressing steel eccentricity from the center of the beam, A is the beam cross-sectional area, and the rest of the variables have been previously defined. The resulting feasible solutions utilizing the above equations are given by the regions inscribed by the four lines in Fig. 2A and 2B, for the AASHTO HS-20 and H-20 truck loadings, respectively. The solutions in these figures are also bound by the physical constraint that the eccentricity e cannot exceed 18.68 in. (the distance from the neutral axis to the beam's bottom minus 3 in. cover). Two solutions were investigated to account for the possibility that the bridge was originally designed for either of the two AASHTO loads.[1,7,8]

Any combination of initial prestress force and eccentricity (P_i and e) falling in the feasible solution region should result in midspan stresses meeting the allowable stress limits. Using any such combination to calculate the stresses $f_{bi\_}$, $f_{ti\_}$, $f_{tf\_}$, and $f_{bf\_}$ in Eq. (8) below at midspan should result in stresses meeting the requirements of Section B3 on the respective stresses f_{bi}, f_{ti}, f_{tf}, and f_{bf}.

$$
\begin{aligned}
f_{bi\_} &:= \frac{P_i}{A} + \frac{P_i \cdot ec}{S_b} - \frac{M_{DL}}{S_b} \\
f_{ti\_} &:= -\frac{P_i}{A} + \frac{P_i \cdot ec}{S_t} - \frac{M_{DL}}{S_t} \\
f_{bf\_} &:= -\frac{\kappa \cdot P_i}{A} - \frac{\kappa \cdot P_i \cdot ec}{S_b} + \frac{M_{Tot}}{S_b} \\
f_{tf\_} &:= \frac{\kappa \cdot P_i}{A} - \frac{\kappa \cdot P_i \cdot ec}{S_t} + \frac{M_{DL}}{S_t}
\end{aligned}
\tag{8}
$$

Two initial prestress force and eccentricity combinations were selected from each of the solutions in Fig. 2. Analysis was then performed for each of those combinations to determine effective prestress force P_e, area of steel A_s, ultimate moment M_u, factored dead load and live load moments M_{Fact}, cracking moment M_{cr}, the moment available for testing M_{Test} and its resulting midspan stress f_{Test}, and the maximum deflection to be expected during the test Δ. The results of this analysis are shown in Table 1. Maximum deflections were calculated for a concentrated midspan load calculated using the test moment and assuming simply supported end conditions. From this analysis the following observations can be made:

1. As expected, the most economical designs, in terms of area of steel, include combinations of low prestressing forces and large eccentricities. One of those combinations was probably used in the bridge design.
2. All combinations resulted in ultimate moments exceeding factored dead load and live load moments. This makes the graphical solution for initial force and eccentricity combinations plausible.

Midspan instrumentation | Melted ice on day of testing

Figure 4. Mounting strain gages at midspan and a photo of the melted ice 1 week later

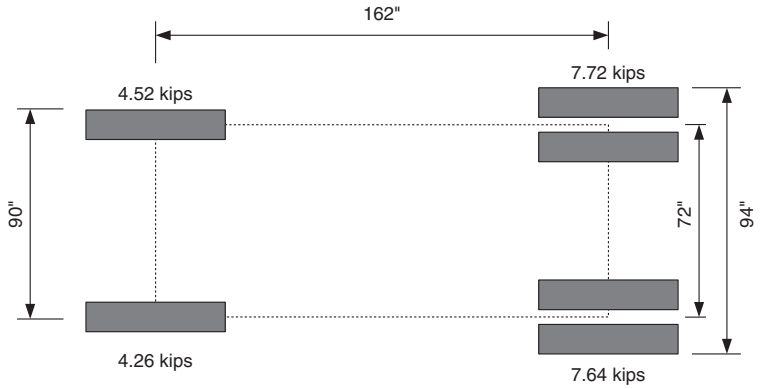

12-Ton Test Vehicle

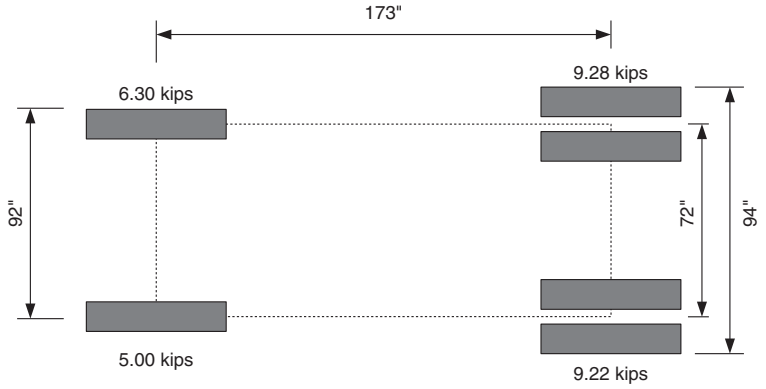

15-Ton Test Vehicle

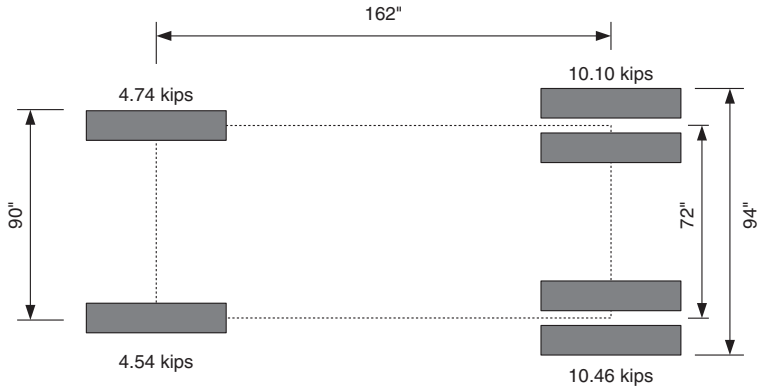

12-Ton Test Vehicle Raised to 15Tons

Test vehicle axle and gross weights

Test Vehicle	Front Axle Wt. (kips)	Rear Axle Wt. (kips)	Gross Vehicle Wt. (kips)
12-ton Truck	8.78	15.36	24.14
15-ton Truck	11.30	18.50	29.80
12-ton Raised to 15-ton	9.28	20.56	29.84

Figure 5. Test vehicle dimensions and wheel and axle loads

3. The lowest moment available for testing is 6.88×10^3 kip-in. (573 kip-ft). This is the moment that would crack a beam if it were fully applied during the testing.

In addition to the above observations, it was also noted that the code requirements on maximum and minimum prestressing steel percentages were satisfied for all four P_i and e combinations.[8]

Instrumentation

The bridge was instrumented at various locations to determine (1) midspan bottom flange stresses for all five beams, (2) level of fixity at the ends of all beams, (3) neutral axis location for the two fascia beams (Beams 1 and 5) and one interior beam (Beam 3), and (4) deflections at midspan of Beams 1 and 5 (fascia beams) and Beam 3.

Strain gages (manufactured by Bridge Diagnostics, Inc.) were used in the instrumentation. Three deflection gages were also planned for midspans of Beams 1, 3, and 5 but were not mounted due to logistics problems. A general-purpose strain gage measurement system, "System 6000" (manufactured by The Measurement Group), was employed for data acquisition. The complete instrumentation plan, including the location of strain gages and proposed LVDT deflection gages, is shown in Fig. 3.

Figure 6. Test vehicle moving into position

At the bridge crossing, the Hannacrois Creek is too deep to use ladders or waders to mount instrumentation at the beams' midspan locations. Additionally, the vertical clearance of the bridge is low. The low clearance combined with the 12-ton posting made use of an under-bridge inspection unit impossible. A decision was made to wait for the river to freeze and instrument the bridge from the ice surface. The thickness of the ice was monitored with an ice drill, and 20 strain gages were mounted on the structure at designated locations (Figs. 3 and 4) from the frozen ice surface. On the day of the testing, warm weather melted the ice and instrumenting the midspans of three girders with deflection gages (LVDTs) was not possible (Fig. 4).

Truck weights and dimensions

Prior to the testing, the test trucks were weighed and axle spacing measured for each truck. When loading the trucks with sand, care was taken to evenly distribute the load in the backs of the trucks. Two trucks were used in the testing—a 12-ton vehicle and a 15-ton vehicle. The loading of the 12-ton truck was increased to 15 tons for the second half of the testing. Dimensions and wheel loads are shown in Fig. 5, axle and gross vehicle weights are also summarized in Fig. 5, and a photo of a test vehicle is shown in Fig. 6. Each of the 15-ton trucks closely resembles an AASHTO H-15 truck.

Load Test Plans

The test plan is divided into four phases based on the loading scenario. Prior to the testing, each scenario was analyzed assuming the structure to be simply supported to determine expected strain levels during the testing. The structure was loaded incrementally by positioning the test trucks in a manner that would gradually increase midspan moment on the structure, while continually monitoring the strain gage readings.

Loading of the structure was calculated to remain below cracking. Inspection reports also did not show cracking in any of the beams. Throughout the load test, the structure was monitored for unexpected cracking, excessive deflection, abnormal strain readings, sensor issues, or other unusual behavior. If the structure did not behave as intended, the load test was stopped immediately. The strategy followed was to proceed to the next phase (increased loading) only when the preceding phase stresses were within expected limits. The following is a full description of the load test plan phases.

Phase 1

The first portion of the testing focuses one axle line of a 12-ton (the current posted weight limit) vehicle on each of the structure's five beams. The vehicle is to cross the bridge at crawl speed, stopping for readings when the rear axle is at each sixth point of the bridge (five readings per load sequence). All crossings begin at the south side of the structure. This phase is expected to reveal relative differences among the beams based on their response to similar loads. Lines indicating the beam centerlines and positions to place the rear axle were painted on the bridge prior to the test date. Illustrations of the truck paths are shown in Figs. 7 and 8. The beams will be tested in the order, Beam 1 through Beam 5. After each beam has been loaded, peak strain readings for each beam will be compared to the estimated safe strain and a decision will accordingly be made to continue with Phase 2 of the testing or not. At the end of this phase of testing, the 12-ton truck will return to a maintenance yard, and the gross weight of the vehicle will be increased to 15 tons.

Phase 2

Phase 2 of the testing uses a 15-ton vehicle that is planned to travel across the bridge at crawl speed stopping with the rear axle at the bridge sixth points for readings. The same

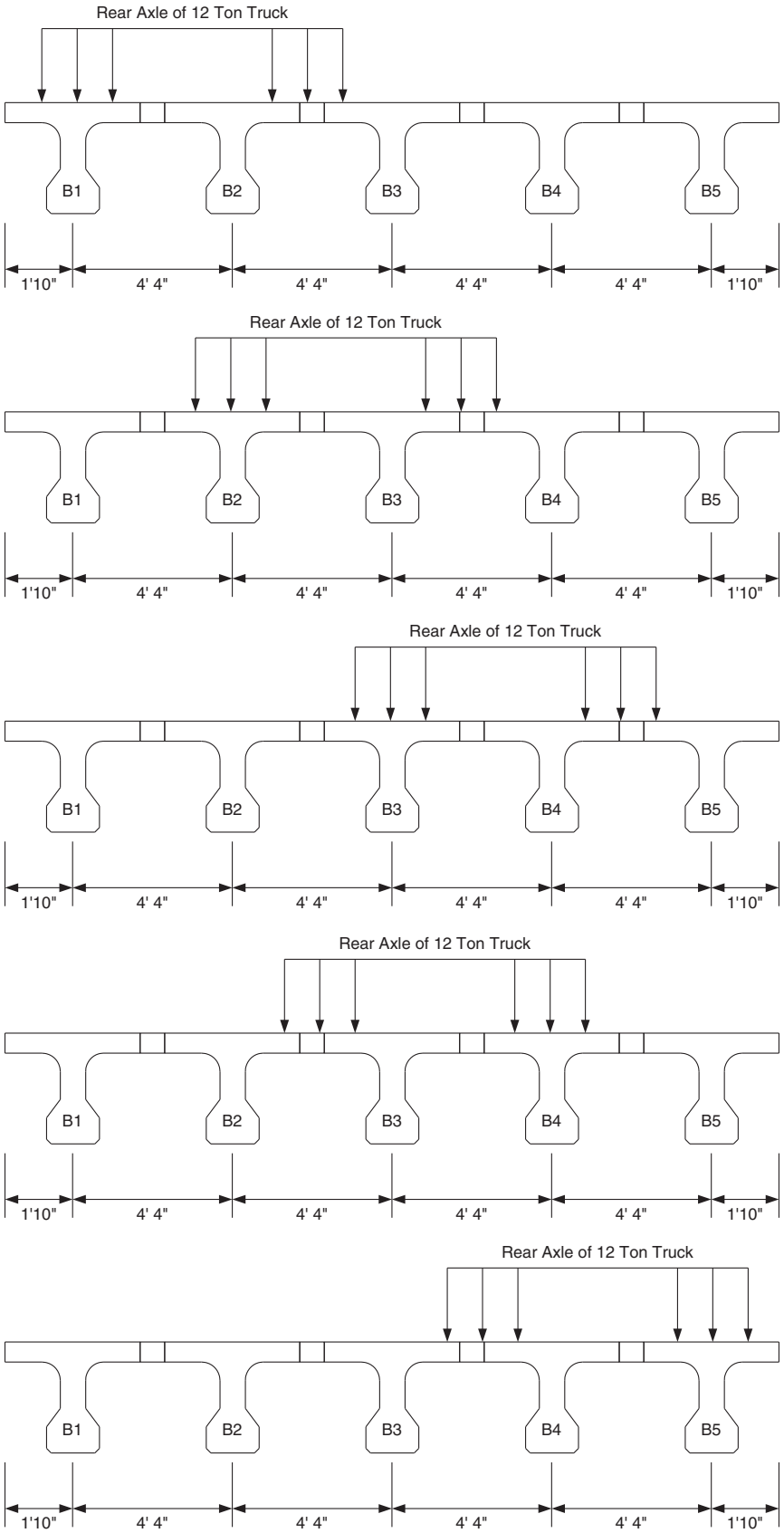

Figure 7. Wheel line locations for Phase 1 (not to scale)

vehicle will cross in the Northbound lane first and then in the Southbound lane. Both crossings begin on the south side of the structure. This phase will provide information on the structure's response for a load slightly higher than

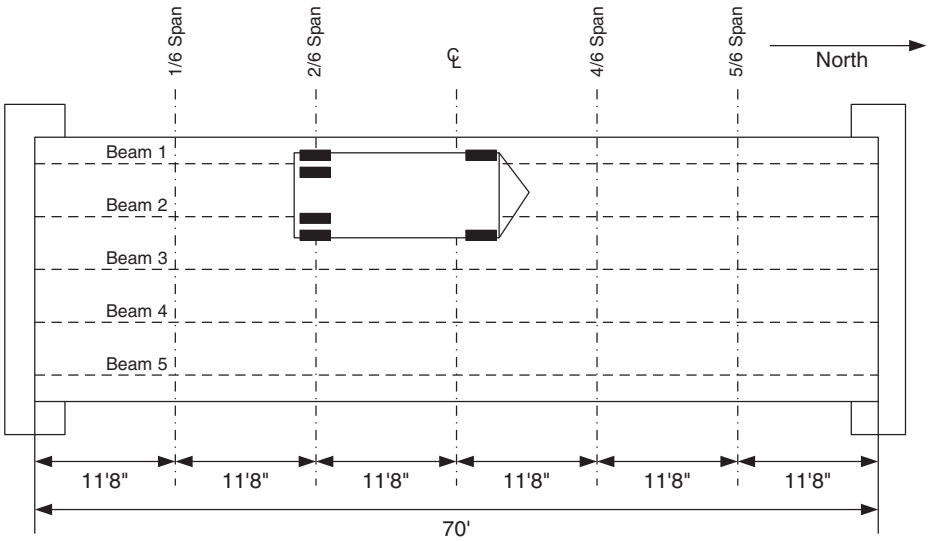

Figure 8. Phase 1 testing. A 12-ton vehicle with a wheel line on Beam 1 is shown stopping at marked locations on the bridge. This is repeated for each beam

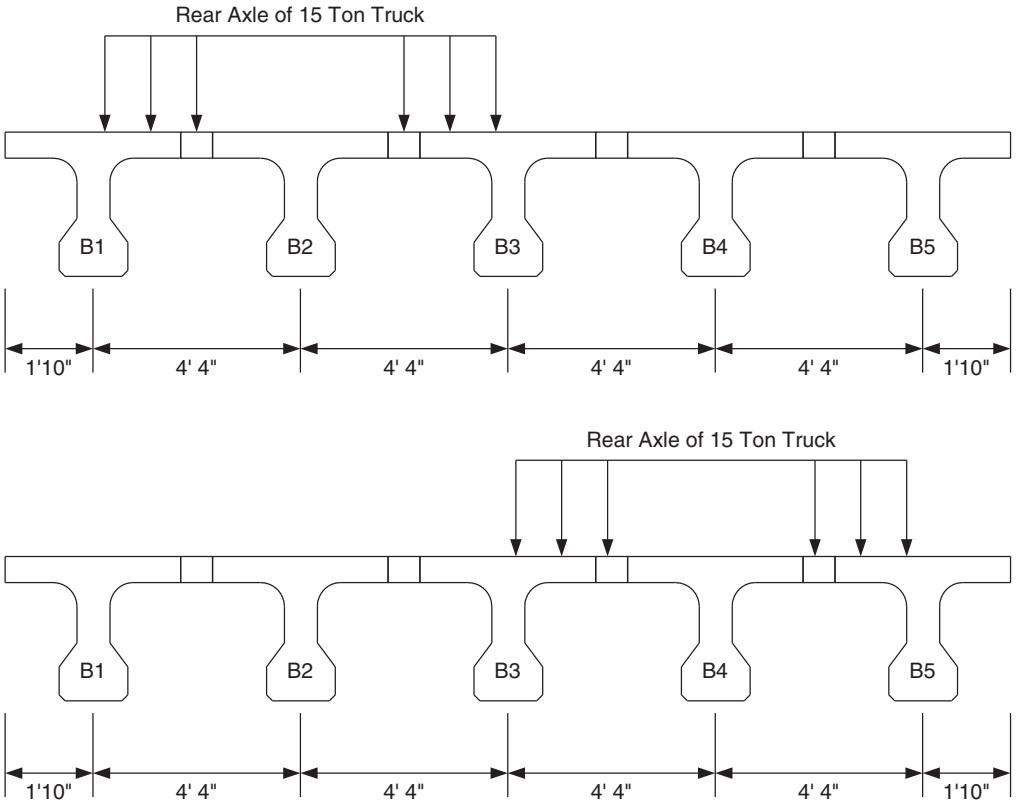

Figure 9. Fifteen-ton vehicle load paths

the posted. The truck paths are shown in Fig. 9. Strain data will be evaluated at each position and if the results are determined to be acceptable, the testing will be continued to Phase 3.

Phase 3

In Phase 3, two 15-ton trucks will be used. The two vehicles will follow each other across the bridge at crawl speeds, without stopping, keeping the following distance between the trucks at approximately 15 ft. The testing will be repeated in the Northbound lane first and then in the Southbound lane. Both crossings begin at the south end of the bridge. This phase will increase the loading on the structure by about 25 percent than that used in Phase 2. Strains will be continuously monitored to determine if the testing should be continued to Phase 4 or not.

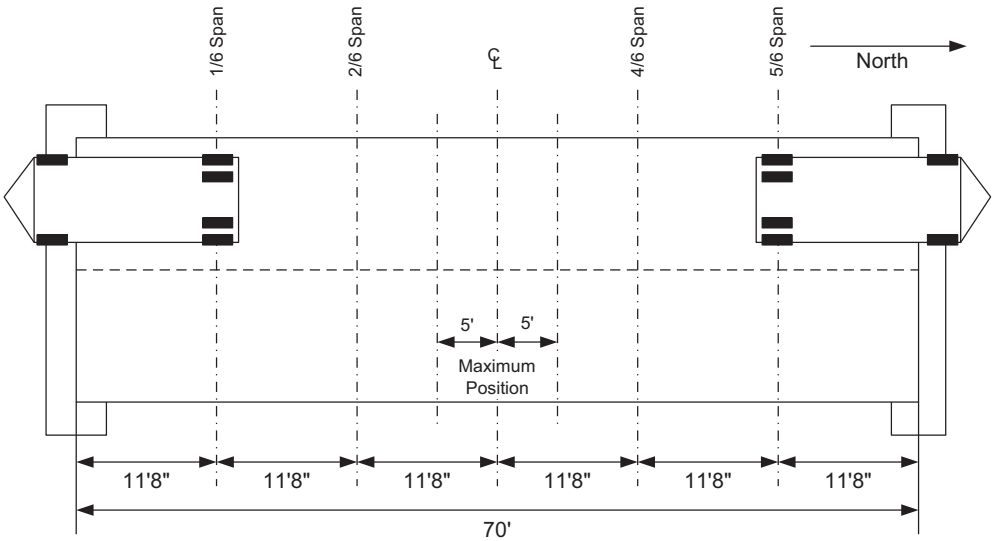

Figure 10. Two 15-ton vehicles back-to-back. (Testing repeated in Northbound lane)

Table 2. Estimated midspan moments and strains on beams during the testing, assuming simply supported end conditions

Test truck	Rear axle position	Predicted bridge moment (kip-ft)	Predicted beam moment (kip-ft)	Predicted strain (με)
12 ton	1/6 Point	197	85	59
12 ton	2/6 Point	319	137	96
12 ton	3/6 Point	365	157	110
12 ton	4/6 Point	223	96	67
12 ton	5/6 Point	93	40	28
15 ton	1/6 Point	246	106	74
15 ton	2/6 Point	398	171	120
15 ton	3/6 Point	456	196	137
15 ton	4/6 Point	287	123	86
15 ton	5/6 Point	117	50	35
Two 15 ton	Following	620	267	187
Two 15-ton back-to-back	1/6 Point	230	99	69
Two 15-ton back-to-back	2/6 Point	568	244	171
Two 15-ton back-to-back	Midspan	763	328	230

Phase 4

The two 15-ton vehicles will be placed back-to-back on the bridge. Testing will begin on the Northbound Lane with the rear axle of each vehicle at a sixth point of the bridge. Strains will be monitored at each step during the test, and if found to be acceptable, the trucks will be brought closer together to the 2/6 span markings, increasing the load effect of the bridge. If the strains at all steps are deemed to be acceptable, the trucks will be brought to a final back-to-back position at midspan to produce the maximum loading that will be applied during the testing. The Phase 4 back-to-back configuration will be repeated in the Southbound Lane. This phase of the testing will produce the highest loading on the structure because the limited bridge width does not allow for a side-by-side testing. The truck positions in this phase are shown in Fig. 10.

Estimated load effects

Prior to the testing, axle spacing for the test trucks was measured (164 in.) and the axle weights had to be estimated. For the 12-ton vehicle, a steering axle weight of 8 kips and a rear axle weight of 16 kips were assumed, and for the 12-ton truck, a steering axle weight of 10 kips and a rear axle weight of 20 kips were assumed. Using a simply supported finite element beam model, gross moments were calculated for each load case and then reduced to the beam level using the AASHTO distribution factor of 0.43. A modulus of elasticity was calculated for concrete based on a 5000-psi compressive strength. Using the estimated modulus, section

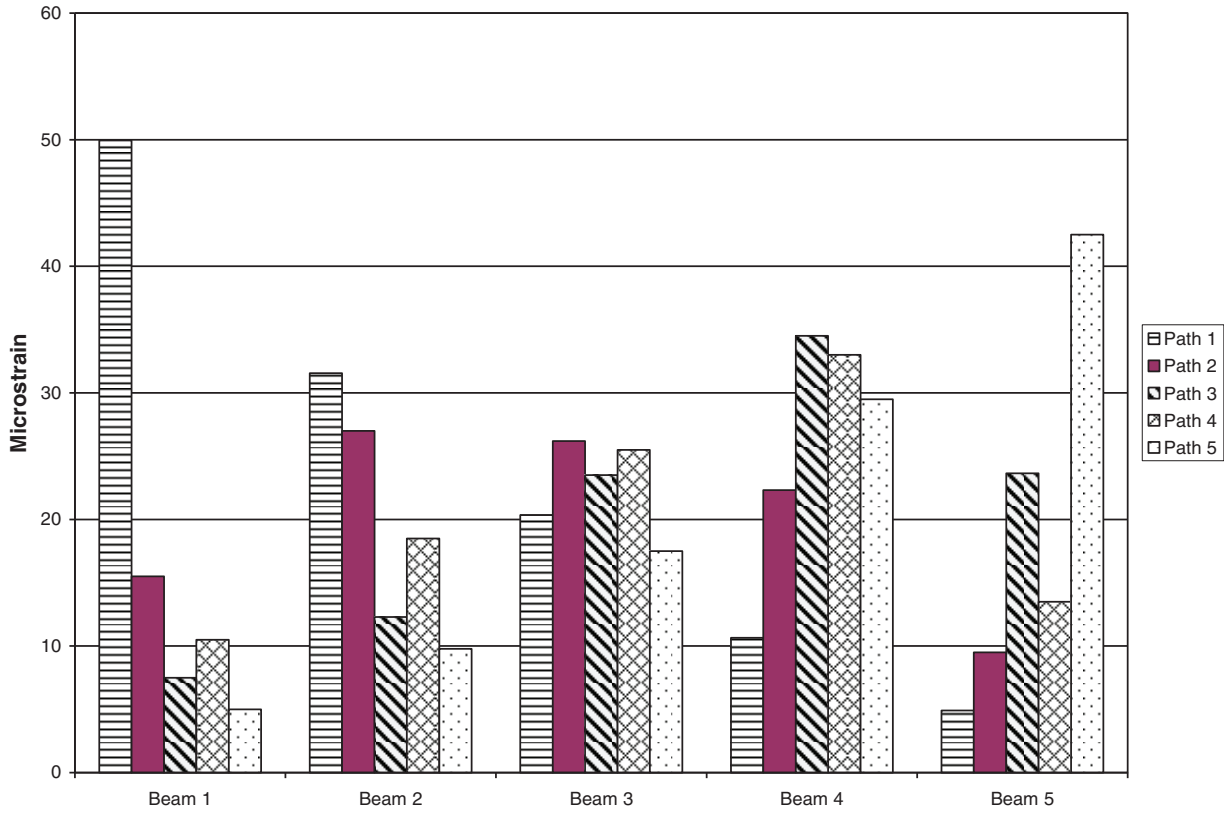

Figure 11. Midspan strain readings for the 12-ton crossings

Table 3. Distribution percentages for the 12-ton crossings

Path number	Beam number				
	1	2	3	4	5
1	42.5	26.9	17.3	9.1	4.2
2	15.4	26.9	26.1	22.2	9.5
3	7.4	12.1	23.2	34.0	23.3
4	10.4	18.3	25.2	32.7	13.4
5	4.8	9.4	16.8	28.3	40.8

properties, and estimated load effects, midspan strain for each load case in the testing was obtained as shown in Table 2.

Analysis of the Test Results

Load distribution

Phase 1 testing included a 12-ton truck aligning a wheel line with each of the five bridge beams. Fig. 11 shows the midspan strains recorded at the midspan point during each truck crossing. In most paths, the beams intentionally being loaded had the peak strain values. The exception is Path 3. In this passing, Beam 4 had the highest peak strain. For Paths 1, 2, and 3 crossings, the driver's side wheel line was placed directly on the beam. For the Paths 4 and 5 crossings, the passenger side wheel load was placed on the beam. Therefore, the Path 3 and Path 4 crossings apply similar loads on Beams 3 and 4. This can be seen in the Phase 1 test plan in Fig. 8. The peak strain in this portion of the testing was 50 με, which is significantly lower than the 110 με predicted in the preliminary analysis.

The percentage of the total moment on the bridge due to the test trucks is calculated by dividing each midspan gage reading by the sum of the five midspan gage readings, assuming all the beams have similar section moduli.

The percentages of the total truck moment carried by each of the beams during the truck crossings at the midspan point are shown in Table 3. As noted earlier, the similarity of Paths 3 and 4 crossings is reflected in the figure. After an on-site review of the low strains and the observed good load distribution, a decision was made to continue with the next phase of the testing.

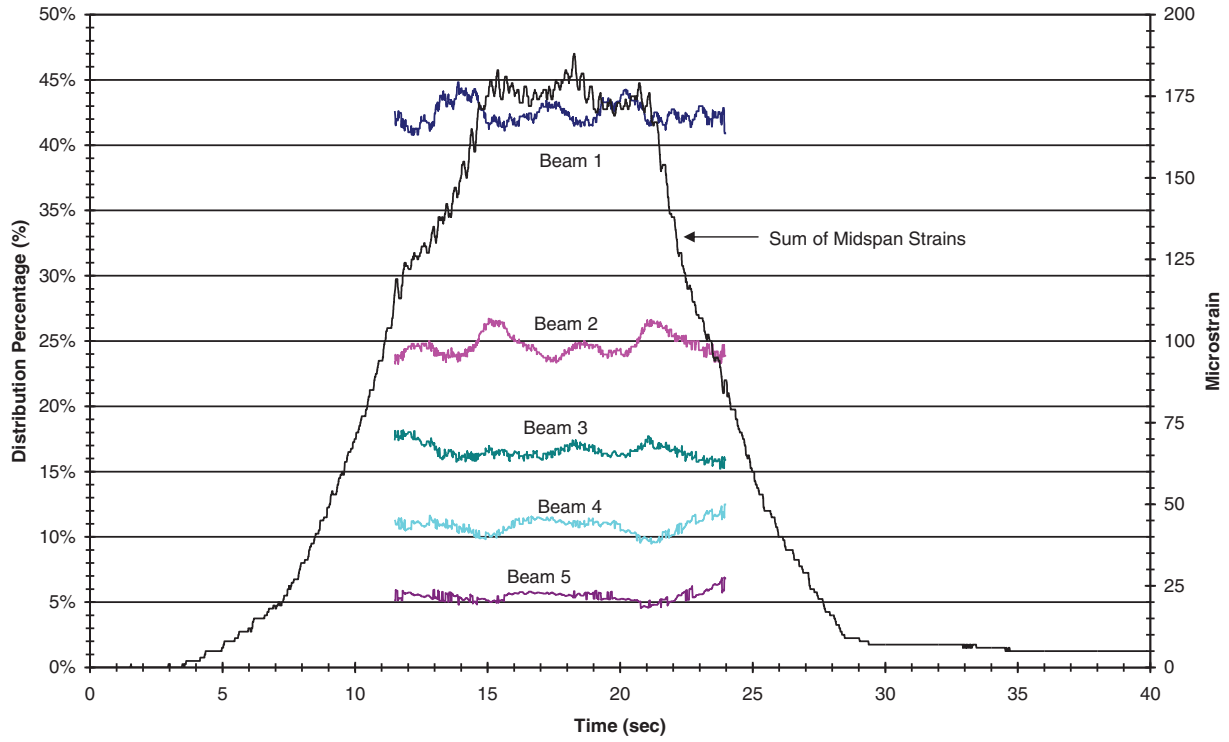

Figure 12. Continuous representation of load distribution percentages for two 15-ton trucks following each other on the upstream lane

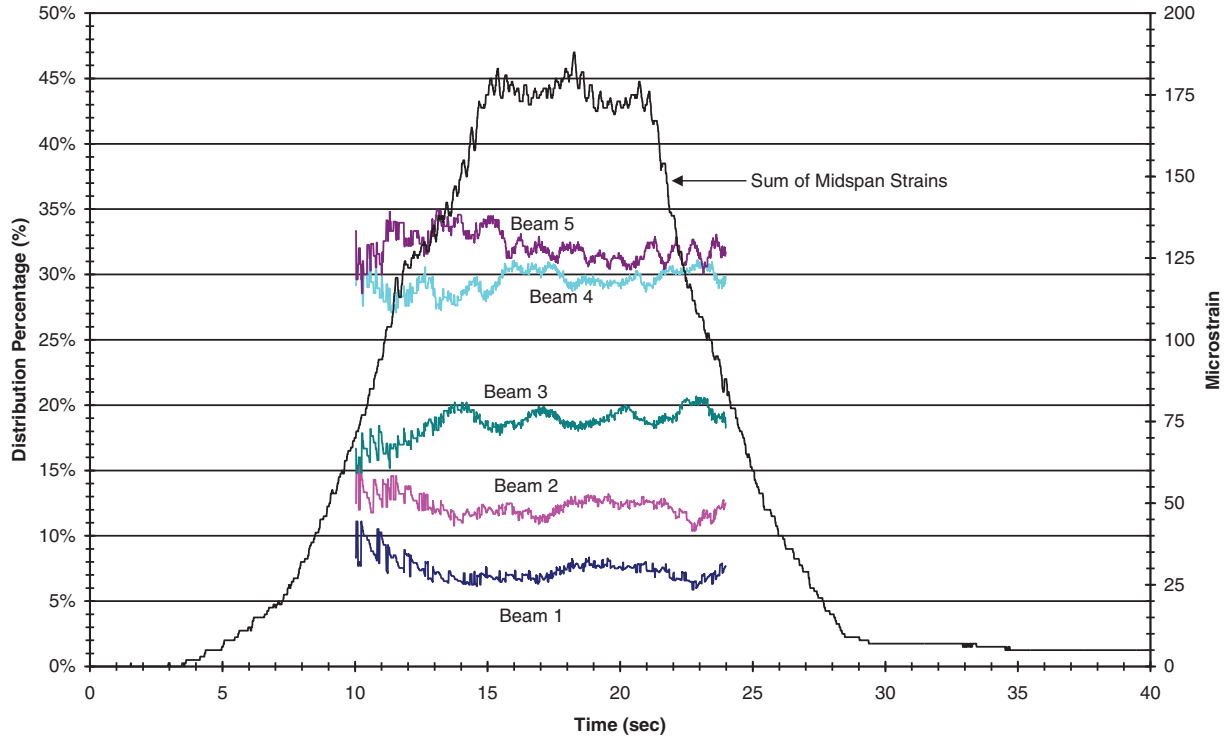

Figure 13. Continuous representation of load distribution percentages for two 15-ton trucks following each other on the downstream lane

Phase 2

The 15-ton truck traveled North twice on each of the upstream and downstream lanes of the structure in this phase. Again, after an on-site review of peak strain readings and the good load distribution between the bridge beams, a decision was made to continue with the next phase of the testing. This phase is intermediary, and for detailed results the reader may refer to.[8]

Figure 14. Icicles from water seeping between beams

Phase 3

This phase of the testing involved two 15-ton trucks following each other at crawl speed without stopping on the structure. The test was repeated on the upstream and downstream lanes, and the time histories for the midspan gages for the two lanes were recorded. Beam moment distribution percentages are obtained using peak strains and are shown in Figs. 12 and 13 using continuous representations. From these figures, Beam 1 is clearly the most loaded beam during the upstream lane crossing, while Beams 4 and 5 were the most loaded beams during the downstream crossing. There are noticeable differences when comparing the time histories and distribution percentages of the upstream and downstream following load cases. The strains under comparable loading measured on Beam 1 are higher than those measured on Beam 5. The highest load percentage calculated from this phase of the testing was also for Beam 1. Several factors could be responsible for these differences. First, the position of the trucks in the lane could have varied. The vehicles could have been very close to the curb near Beam 1 during the upstream crossing and further away from Beam 5 curb during the downstream crossing. Higher strain readings are sometimes indicative of a low section modulus or poor load distribution; however, these are unlikely based on the results of the previous phases. The joints on the sides of both fascia beams, along the closure pours, showed deterioration that allows for water seepage and formation of icicles (Fig. 14). Based on the low strain readings and good load distribution, the testing continued with positioning the two 15-ton trucks back-to-back as planned in Phase 4 testing.

Phase 4

This phase of the testing included loading of the structure on the upstream and downstream lanes, one lane at a time, with two trucks positioned back-to-back and moved in steps towards the bridge midspan. Midspan strain results are shown in Figs. 15 and 16 for the upstream and downstream lanes, respectively. The heaviest load case, "Mid" with the rear axles approximately 5 feet from midspan, places 763 kip-ft in a lane which is greater than an H-20 lane loading for a 66 ft span (clear span). The peak reading under this loading was 117 με and again, it was on Beam 1. Load distribution patterns for all the back-to-back load cases are similar to those found in the earlier testing.[7]

The strain results for the maximum loading position during this phase of testing were used to generate the comparative load percentage plots shown in Figs. 17 and 18, comparing midspan values to those recorded at the beam ends. The end span percentages are generally within 10 percent of those obtained for the midspan location.

Neutral axis location

Gages were placed on the bottom flange at all midspan beam locations, with additional top flange gages placed on Beams 1, 3, and 5. With the distance between the top and bottom gages known (29.5 in.), the neutral axis of the beam was calculated. The neutral axis of the beam estimated based on the beam's dimensions is 21.668 inches from the bottom. Using the data recorded from the static loadings, the average neutral axis locations for Beams 1, 3, and 5 were calculated in Table 4. Using the six back-to-back position results, the neutral axis locations were also calculated for Beams 1, 3, and 5.

Further analysis of the test results revealed that Beam 5 was about 10% weaker/of lesser stiffness than the remaining beams and that the maximum moment recorded during the load testing was about 50 percent of that estimated prior to the testing.[8] Since the beams are similar in geometry, deterioration of the top part of the beam would be a likely explanation of the reduced stiffness and lowered neutral axis location.

End fixity investigation

This was first investigated by studying how the recorded strains on each of the beams related to the truck moments on the structure, assuming simply supported and fixed end conditions. The results of this investigation showed that the beams were acting more like being fixed at their ends than being simply supported. Further investigation to determine the level of fixity at the beam's ends concluded that the bridge experienced 90 and 76 percent fixity at the south and north abutments, respectively.[8]

Load Rating Analysis

Based on the findings presented in the previous section, the following decisions were made:

1. Calculate live load moments using the AASHTO distribution factor (S/5, giving an equivalent percentage of about 43 percent) instead of that determined based on the test results (about 47 percent). The higher test distribution percentage was calculated by combining crossings to derive a percentage based on two lanes being loaded. The narrow bridge width does not allow for the presence of more than one large truck on the bridge. The AASHTO distribution factor agrees well with the field-measured distribution percentage with one lane loaded.

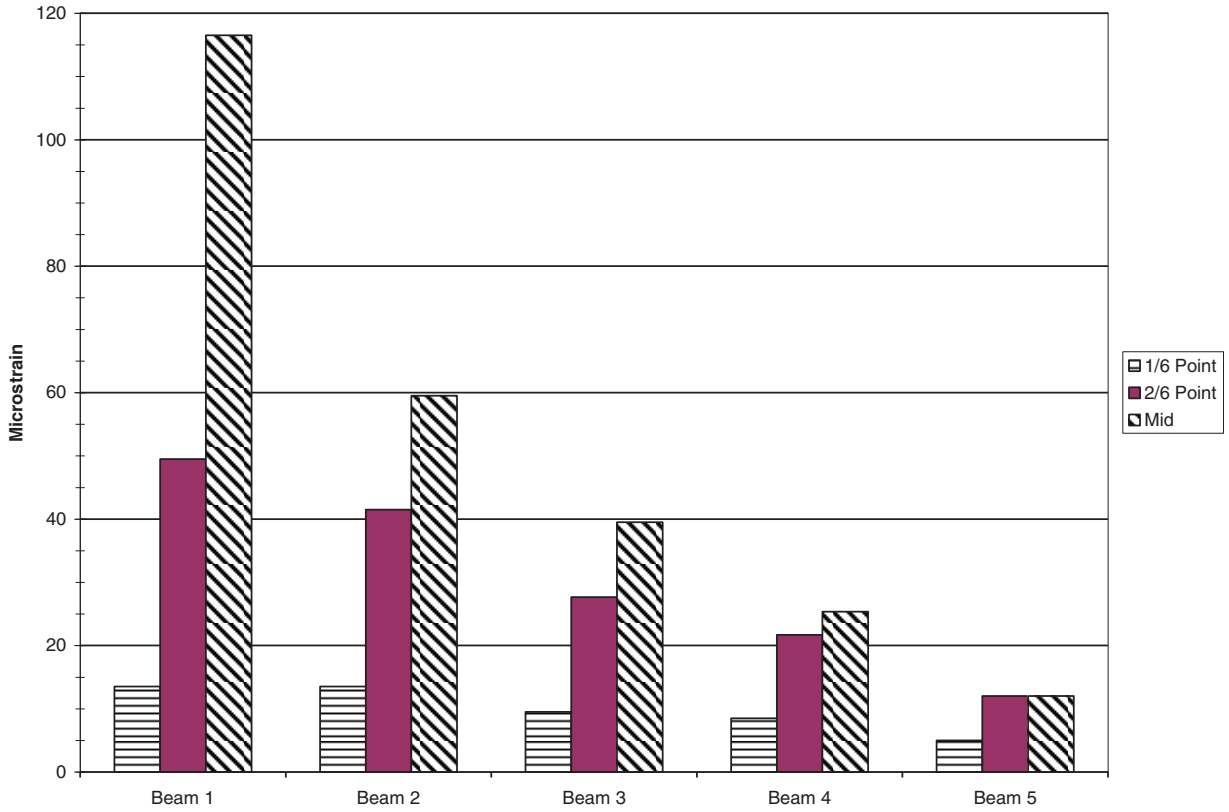

Figure 15. Upstream lane back-to-back midspan strain results

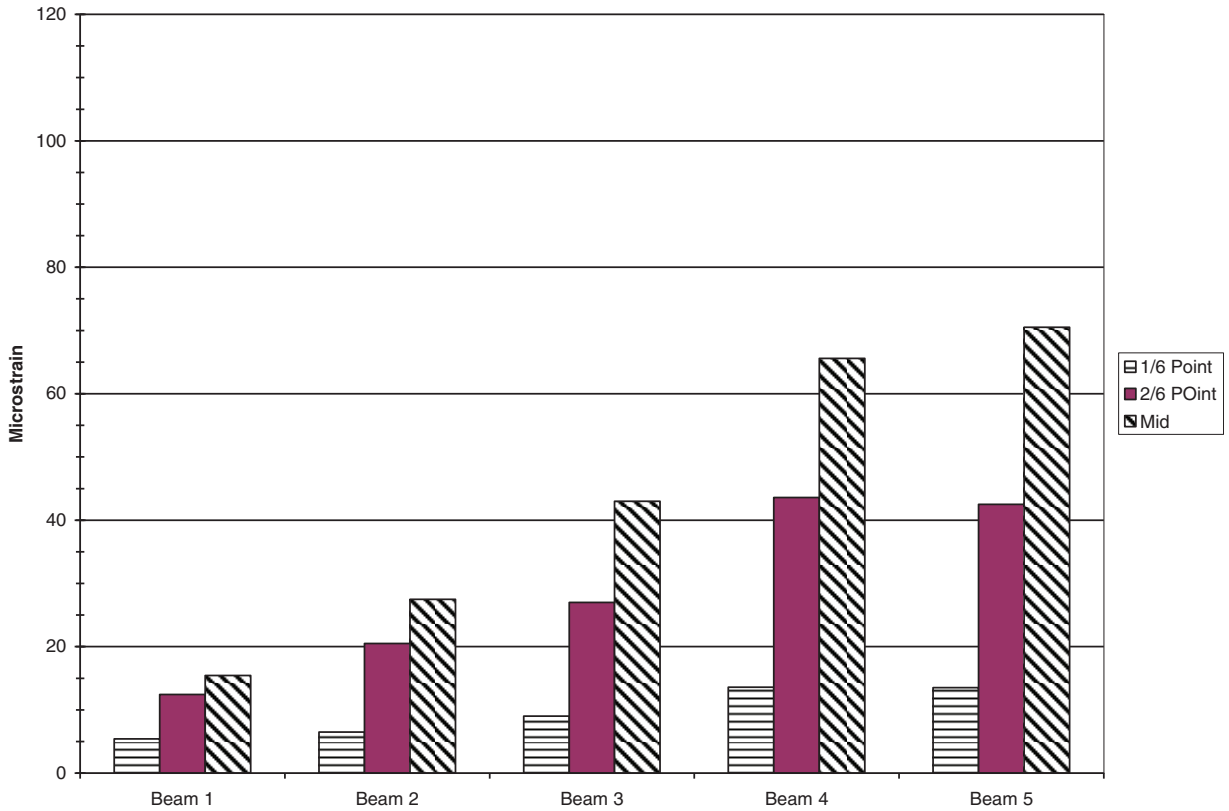

Figure 16. Downstream lane back-to-back midspan strain results

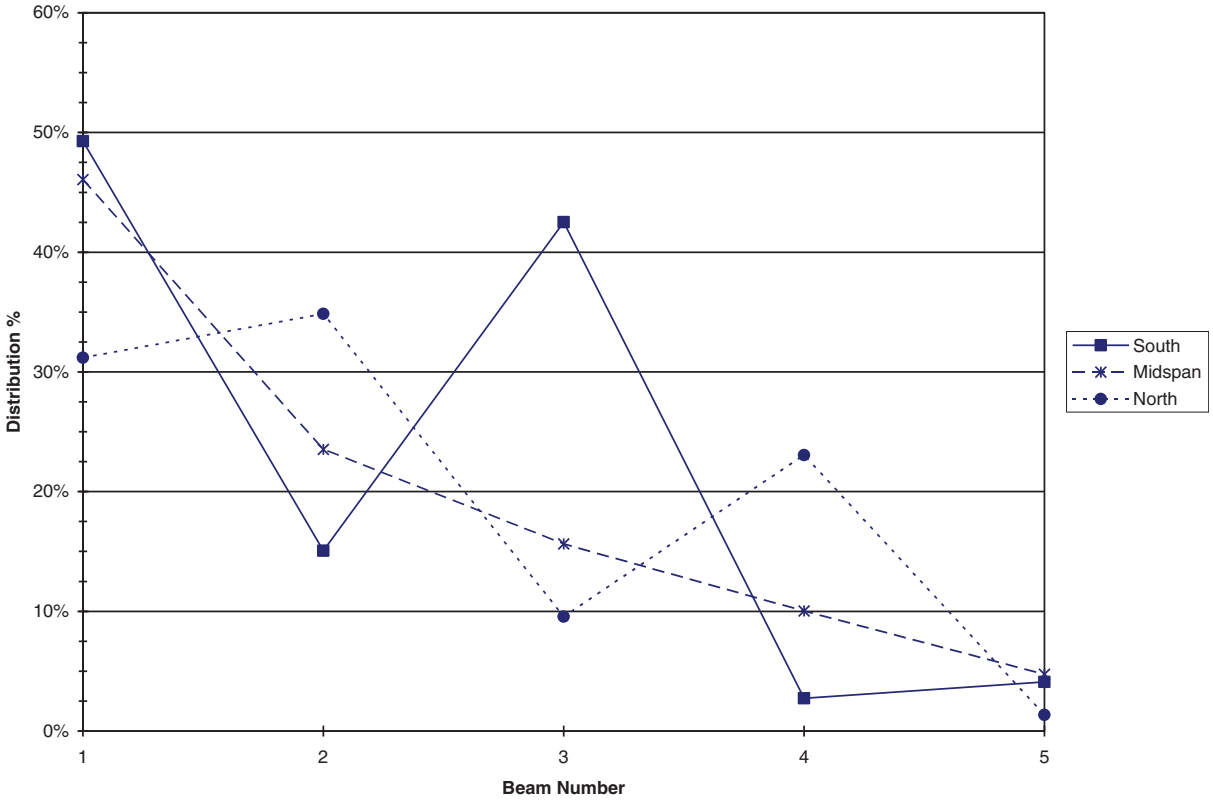

Figure 17. Load distribution percentages: Midspan versus ends for 15-ton truck back-to-back at maximum loading position on upstream lane

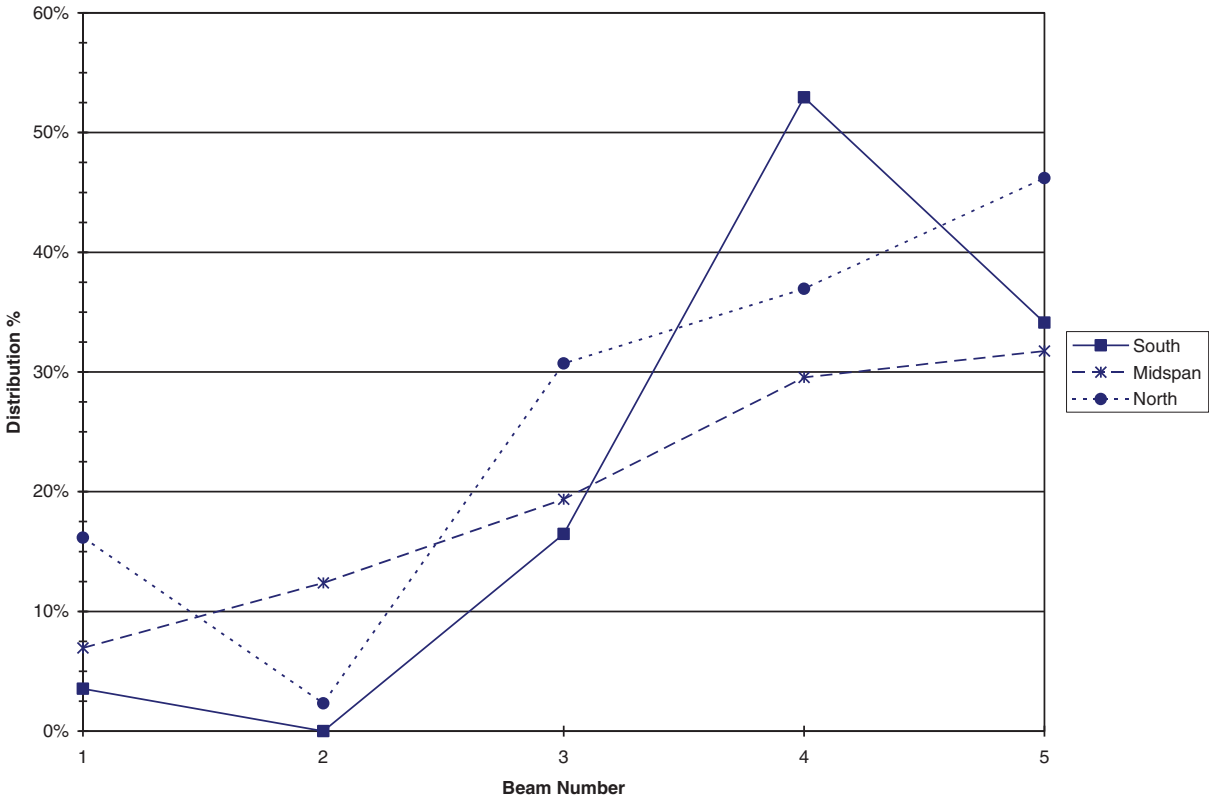

Figure 18. Load distribution percentages: Midspan versus ends for 15-ton truck back-to-back at maximum loading position on downstream lane

Table 4. Average midspan neutral axis locations (measured from beam bottom)

Beam number	Average midspan neutral axis location
1 and 3	22.8 in.
5	19.5 in.

2. Calculate stresses based on a typical (theoretical) section modulus, which is close to that based on the test results.
3. Conservatively ignore fixity in the rating analysis because there is uncertainty in the bridge design, and fixity assumptions may not remain valid at higher loads.

Load rating analysis performed based on the above and identified design parameters resulted in inventory and operating ratings of about 24.6 and 40.8 tons, respectively. The analysis was based on the AASHTO LFD method, including impact. Note that HS-20 and H-20 rating trucks were assumed in the load rating analysis, with each loading scenario accounting for the two possibilities of the bridge being designed using "High P/T" and "Low P/T". See Reference *8* for more information on high and low post-tensioning forces.

Based on the load rating results, the bridge owner was notified of the adequacy of the structure to carry the 15-ton school bus.

Conclusions and Recommendations

This paper introduces a pioneering approach for load rating existing simple-span prestressed concrete bridges with no record plans. To address the data knowledge gap, the approach assumes the structure was originally designed to the minimum AASHTO code requirements applicable at the time of construction. It then uses a linear programming solution to establish feasible combinations of prestressing force and eccentricity information. Finally, it utilizes the results in full-scale load testing to investigate the bridge response to loads and determine parameters for safe and reliable load rating of the structure. The documented approach serves as a proven evaluation tool and has already been validated in subsequent related studies.[9,13]

The paper showed how load testing could be planned and performed, despite the lack of design information about the structure. The incremental approach to the testing and the type of reasoning and analysis described in the paper could be replicated on any simple-span prestressed concrete structure with no plans on record.

The primary findings from the load testing can be summarized as follows:

- a. Load distribution on the structure was excellent and comparable with that estimated using the AASHTO equation.
- b. The theoretical beam section modulus was verified using results based on strain readings from gages mounted to determine neutral axis locations and again from moment-versus-strain results.
- c. The structure was about 90 percent fixed at the south end and about 76 percent fixed at the north end.
- d. An AASHTO LFD load rating was performed using a conservative approach, assuming the structure to be simply supported, the actual AASHTO distribution factor, and the theoretical section modulus, which was very close to that based on the test results.
- The recommended H inventory and operating ratings are 24.6 and 40.8 tons, respectively, and the recommended HS inventory and operating ratings are 40.3 and 67.7 tons, respectively
- e. The structure is more than adequate for carrying a15-ton school bus traffic.

Acknowledegments

Instrumentation and data collection for this project were conducted by George Schongar and Harry Greenberg, previously with the NYSDOT Research Bureau. The coordination and assistance of the Greene County Highway Department staff are gratefully acknowledged. All the views represented in this paper are those of the authors and not necessarily those of the NYSDOT.

References

[1] *Manual for Bridge Evaluation*. 3rd ed. Washington, D.C: American Association of State Highway and Transportation Officials; 2018.

[2] Alampalli S, Hag-Elsafi O. Sensors and instrumentation for bridge testing. *40th International Instrumentation Symposium, Instrumentation Society of America*; May 1994; Baltimore, Maryland, 485–496.

[3] Hag-Elsafi O, Kunin J, Alampalli S. Evaluating effectiveness of FRP composites for bridge rehabilitation through load testing. *Structural Materials Technology: An NDT Conference*; February–March 2000; Atlantic City, NJ, 434–439.

[4] Hag-Elsafi O, Alampalli S, Kunin J. In-service evaluation of a reinforced concrete T-beam bridge FRP strengthening system. *J Compos Struct, Elsevier Sci*. 2004;64(2):179–188. doi:10.1016/j.compstruct.2003.08.002.

[5] Alampalli S, Lund R. Field testing to determine the remaining fatigue life of patroon Island bridge. *ASNT Fall Conference & Quality Testing Show*; November 2004; Las Vegas, NV.

[6] Alampalli S, Hag-Elsafi O. Load testing of bridge FRP applications. *Chapter 40, International Handbook of FRP Composites in Civil Engineering*; September 2013; CRC Press.

[7] *Standard Specifications for Highway Bridges*. Washington, D.C: Association of State Highway and Transportation Officials; 1961.
[8] Hag-Elsafi O, Kunin J. *Load Testing for Bridge Rating: Dean's Mill Over Hannacrois Creek, Special Report 147*. Albany, NY: Transportation R&D Bureau, New York State Department of Transportation; February 2006.
[9] Aguilar CV, Jauregui DV, Newtson CM, Weldon BD, Cortez TM. Load rating a prestressed concrete double T-beam bridge without plans for field testing. In: *Transportation Research Record*. Washington, D.C: Transportation Research Board; 2015.
[10] Shenton HW III, Chajes MJ, Huang J, Load rating of bridges without plans. In: *Final Report DCT 195*. Delaware Center for Transportation, Dover; 2007.
[11] *Bridge Inspection Manual*. Austin, TX: Texas Department of Transportation (TxDOT); 2024.
[12] *ODOT LRFR Manual*. Salem, OR: Oregon Department of Transportation (ODOT); 2018.
[13] Jáuregui DV, Newtson CM, Weldon BD et al. Load rating bridges with no as-built plans or non-engineered bridges. In: *Report NM13STR-01*. 3035 S. Espina Street, Las Cruces, NM 88003: New Mexico State University, Department of Civil Engineering; June 2015.